Kinetic and Structural Investigations of the Allosteric Site in Human Epithelial 15-Lipoxygenase-2[†]

Aaron T. Wecksler,[‡] Victor Kenyon,[‡] Natalie K. Garcia,[‡] Joshua D. Deschamps,[‡,§] Wilfred A. van der Donk,[⊥] and Theodore R. Holman*,[‡]

[‡]*Chemistry and Biochemistry Department, University of California, Santa Cruz, California 95064, and* [⊥]*Department of Chemistry, University of Illinois at Urbana−Champaign, 600 South Mathews Avenue, Urbana, Illinois 61801*[§]*Current address: KaloBios Pharmaceuticals, Inc., 260 East Grand Ave., California 94080, USA*

ABSTRACT: Allosteric regulation of human lipoxygenase (hLO) activity has recently been implicated in the cellular biology of prostate cancer. In the current work, we present isotope effect, pH, and substrate inhibitor data of epithelial 15-hLO-2, which probe the allosteric effects on its mechanistic behavior. The $^D k_{cat}/K_M$ for 15-hLO-2, with AA and LA as substrate, is large indicating hydrogen atom abstraction is the principle rate-determining step, involving a tunneling mechanism for both substrates. For AA, there are multiple rate determining steps (RDS) at both high and low temperatures, with both diffusion and hydrogen bonding rearrangements contributing at high temperature, but only hydrogen bonding rearrangements contributing at low temperature. The observed kinetic dependency on the hydrogen bonding rearrangement is eliminated upon addition of the allosteric effector, 13-(S)-hydroxyoctadecadienoic acid (13-HODE), and no allosteric effects were seen on diffusion or hydrogen atom abstraction. The $(k_{cat}/K_M)^{AA}/(k_{cat}/K_M)^{LA}$ ratio was observed to have a pH dependence, which was fit with a titration curve (pK_a = 7.7), suggesting the protonation of a histidine residue, which could hydrogen bond with the carboxylate of 13-HODE. Assuming this interaction, 13-HODE was docked to the solvent exposed histidines of a 15-hLO-2 homology model and found to bind well with H627, suggesting a potential location for the allosteric site. Utilizing d_{31}-LA as an inhibitor, it was demonstrated that the binding of d_{31}-LA to the allosteric site changes the conformation of 15-hLO-2 such that the affinity for substrate increases. This result suggests that allosteric binding locks the enzyme into a catalytically competent state, which facilitates binding of LA and decreases the $(k_{cat}/K_M)^{AA}/(k_{cat}/K_M)^{LA}$ ratio. Finally, the magnitude of the 13-HODE K_D for 15-hLO-2 is over 200-fold lower than that of 13-HODE for 15-hLO-1, changing the substrate specificity of 15-hLO-2 to 1.9. This would alter the LO product distribution and increase the production of the pro-tumorigenic, 13-HODE, possibly representing a pro-tumorigenic feedback loop for 13-HODE and 15-hLO-2.

Inflammatory response in humans is regulated by fatty acid signaling cascades which are initiated by the hydroperoxidation of polyunsaturated fatty acids. This oxidation is accomplished by three classes of enzymes, cyclooxygenase (COX)[1] (*1*), cytochrome P450 (*2*), and human lipoxygenases (hLO) (*3*), the latter of which is the focus of this study. Lipoxygenases (LO) are a family of iron containing metalloenzymes, which utilize a nonheme catalytic center to incorporate molecular oxygen into a variety of fatty acids. There are three main LOs of pharmacological importance, 5-hLO, 12-hLO, and 15-hLO, which are named according to the position at which oxygen reacts with arachidonic acid (AA) (*4*). The peroxidation of AA by LO results in their respective hydroperoxyeicosatetraenoic acid (HPETE) products (*5*), which are not only responsible for maintaining the homeostasis of the inflammatory response (*6*), but have also been implicated in human diseases, such as asthma, psoriasis, atherosclerosis, and cancer (*7−10*).

Recently, the issue of allostery has become more prominent in the functional discussion of LO. Allostery for lipoxygenase was first demonstrated with 5-hLO, which was shown to possess secondary binding sites for both ATP and Ca^{2+} (*11*). Kinetic studies have demonstrated that calcium is required for catalytic activity, while the binding of ATP synergistically increases the catalytic activity of calcium-bound enzyme (*12−14*). Soybean lipoxygenase-1 (sLO-1) and reticulocyte human 15-lipoxygenase

[1]Abbreviations: LO, lipoxygenase; sLO-1, soybean lipoxygenase-1; 15-hLO-2, human epithelial 15-lipoxygenase-2; 15-hLO-1, human reticulocyte 15-lipoxygenase-1; 12-hLO, human platelet 12-lipoxygenase; COX, cyclooxygenase; AA, arachidonic acid; 15-HPETE, 15-(S)-hydroperoxyeicosatetraenoic acid; 15-HETE, 15-(S)-hydroxyeicosatetraenoic acid; 12-HPETE, 12-(S)-hydroperoxyeicosatetraenoic acid; 12-HETE, 12-(S)-hydroxyeicosatetraenoic acid; d_4-AA, (10,10,13,13)-d_4-AA; LA, linoleic acid; d_{31}-LA, fully deuterated LA; 13-HPODE, 13-(S)-hydroperoxyoctadecadienoic acid; 13-HODE, 13-(S)-hydroxyoctadecadienoic acid; perdeuterated 13-HPODE, fully deuterated 13-(S)-HPODE; perdeuterated 13-HODE, fully deuterated 13-(S)-HODE; k_{cat}, the rate constant for product release; k_{cat}/K_M, the rate constant for fatty acid capture; $k_{cat}/K_M[O_2]$, the rate constant for oxygen capture; KIE, kinetic isotope effect; SIE, solvent isotope effect; $^D k_{cat}/K_M$, kinetic isotope effect for k_{cat}/K_M; $^D k_{cat}$, kinetic isotope effect for k_{cat}; RDS, rate determining steps; RNR, ribonucleotide reductase; dNTPs, deoxyribonucleoside triphosphates; ATP, adenosine triphosphate.

(15-hLO-1) also have allosteric binding sites, as demonstrated by kinetic studies using the synthetic fatty sulfate, oleyl sulfate (OS) (*15*). This work demonstrated that OS binds with considerable affinity to an allosteric binding site on both sLO-1 ($K_D = 0.6 \mu$M) and 15-hLO-1 ($K_D = 0.4 \mu$M), as seen by an increase in the kinetic isotope effect (KIE) of both enzymes in a saturating manner, which mirrored their inhibition curves (*15*). Further stopped-flow experiments demonstrated that binding of OS to sLO-1 did not interfere with enzyme activation, indicating that the allosteric site was not in the active site (*16*). The function of the allosteric site in 5-hLO appears to regulate activity with endogenous ligands, but since no endogenous allosteric effectors have been found for 15-hLO-1, the biological role of the allosteric site in 15-hLO-1 remains unclear.

The substrate specificity of 15-hLO-1 and epithelial human 15-lipoxygenase (15-hLO-2) has been suggested to play a role in prostate cancer since their products of AA and linoleic acid (LA) have different cellular responses (*17−19*). This fact, along with the capabilities of these LO isozymes to catalyze peroxidation of multiple substrates, led us to hypothesize that the function of the allosteric site may be to regulate substrate specificity. To investigate this hypothesis further, a competitive substrate capture experiment was developed which accurately monitored the substrate specificity by having both substrates present in the enzymatic assay (*20*). These experiments lead to the discovery of an allosteric, product-feedback mechanism in which the LO products directly affected the substrate specificity for both 15-hLO-1 and 15-hLO-2. Although allostery is commonly used to regulate protein activity, there are few examples in the literature that demonstrate allosteric regulation of substrate specificity. Ribonucleotide reductase (RNR) is one of the few enzymes that regulate substrate specificity through allosteric regulation (*21*). RNR synthesizes all four deoxyribonucleoside triphosphates (dNTPs) by reduction of the 2′-OH of the respective ribonucleotide, and the ability of RNR to allosterically regulate substrate specificity enables it to maintain homeostatic balance of all four dNTPs, and allow rapid adaptation to changes in dNTP requirements needed for DNA replication and repair. For 15-hLO-1 and 15-hLO-2, the magnitude of the allosteric effects on substrate specificity for LO were of a magnitude similar to that seen for RNR (*22*), and the concentration of the LO products found in the cell were appropriate to elicit a substrate specificity change for 15-hLO-1 (*23*), indicating that the allosteric site may have relevancy for cellular function.

The nature of the allosteric site in 15-hLO-1 was further investigated with isotopic effect experiments, which determined that the allosteric effector lowered the rate-limiting nature of a solvent-dependent, hydrogen bond rearrangement step for the reaction with AA, consequently increasing the relative importance of the hydrogen atom abstraction to the overall kinetics (*24*). This was a significant result suggesting that allosteric binding may regulate substrate specificity by differentially affecting the microscopic rate constants of 15-hLO-1, depending on the substrate.

In the present study, we have expanded our allosteric site investigations to probe the allosteric effects on the mechanistic behavior of 15-hLO-2 with AA, and demonstrate that allosteric product binding influences the rate-limiting contributions of the solvent-dependent, hydrogen bond rearrangement step, as previously seen for 15-hLO-1. The allosteric binding of the effector molecule, 13-(*S*)-hydroxyoctadecadienoic acid (13-HODE), also increases the binding affinity of LA to 15-hLO-2, corroborating

our previous results that showed 13-HODE increasing the k_{cat}/K_M of LA. In addition, we demonstrate that the allosteric binding is pH dependent, with a pK_a of 7.7, suggesting a charge interaction between 13-HODE and a His residue. Docking 13-HODE to our 15-hLO-2 homology model, we rationally hypothesize an allosteric binding site between the two domains of 15-hLO-2 that contains a charged His residue.

MATERIALS AND METHODS

Materials. All commercial fatty acids (Sigma-Aldrich Chemical Co.) were repurified using a Higgins HAIsil Semi-Preparative (5 μm, 250 × 10 mm) C-18 column. Solution A was 99.9% MeOH and 0.1% acetic acid; solution B was 99.9% H_2O and 0.1% acetic acid. An isocratic elution of 85% A:15% B was used to purify all fatty acids, which were stored at −80 °C for a maximum of 6 months. LO products were generated by reacting substrate with the appropriate LO isozyme (13-HPODE from sLO-1 and LA, 15-HPETE from sLO-1 and AA, and 12-HPETE from 12-hLO and AA). Product generation was performed as follows. An assay of 100 mL of 50−100 μM substrate was run to completion, extracted twice with 300 mL of dichloromethane, evaporated to dryness, and reconstituted in MeOH for HPLC purification. The products were HPLC purified using an isocratic elution of 75% A:25% B, as described above for the fatty acid purification. All products were tested with enzyme to show that no residual substrate was present, as well as tested using both analytical HPLC and LC-MS/MS, demonstrating greater than 98% purity. The reduced products were purified similarly; however, trimethylphosphite was added to selectively reduce the peroxide to the alcohol moiety prior to purification. Purified hydroxy products were then tested for purity by HPLC and with enzyme to ensure no loss of lag phase by activation from residual hydroperoxide product. Perdeuterated LA (d_{31}-LA) (98% deuterated, Cambridge Isotope Laboratories) was purified as previously described (*25*). The (10,10,13,13)-d_4-AA (d_4-AA) was synthesized as previously described (*26−28*). All other chemicals were reagent grade or better and were used without further purification.

Overexpression and Purification of Epithelial 15-Human Lipoxygenase-2. Human prostate epithelial 15-lipoxygenase-2 (15-hLO-2), without a His$_6$-tag, was expressed and purified as previously published (*29*). All enzymes were purified to greater than 90% purity, as evaluated by SDS−PAGE analysis. Iron content of 15-hLO-2 was determined with a Finnigan inductively coupled plasma mass spectrometer (ICP-MS), using cobalt-EDTA as an internal standard. Iron concentrations were compared to standardized iron solutions.

Steady-State Kinetic Measurements. Lipoxygenase rates were determined by following the formation of the conjugated diene product at 234 nm ($\varepsilon = 25\,000$ M^{-1} cm^{-1}) with a Perkin-Elmer Lambda 40 UV/vis. All reactions were 2 mL in volume and constantly stirred using a magnetic stir bar in 25 mM HEPES buffer with substrate concentrations ranging from 1 μM to 20 μM. The pH dependency (pH 7−8) and temperature dependency (15−37 °C) on the steady-state kinetics of 15-hLO-2 were determined as previously described (*20*). Assays were initiated with 15-hLO-2 (200−500 nM, normalized to iron content) and all substrate concentrations were quantitatively determined by allowing the enzymatic reaction to go to completion. Kinetic data were obtained by recording initial enzymatic rates at each substrate concentration which were then fitted to the

Michaelis−Menten equation using KaleidaGraph (Synergy) to determine k_{cat} and k_{cat}/K_M values.

Temperature and pH Dependency on the Substrate Specificity using the Competitive Substrate Capture Method. The competitive substrate capture method experiments were performed as previously described (*20*). Briefly, reaction mixtures of AA:LA of known molar ratio (1:1) were initiated with 15-hLO-2 (∼20 nM, normalized to iron content). The ratio of the simultaneous product formation (15-HPETE and 13-HPODE) by 15-hLO-2 was determined at 1 μM total substrate concentration (7-fold less than the K_M of 15-hLO-2 with AA). The reaction was monitored at 234 nm with a Perkin-Elmer Lambda 40 and quenched with acetic acid, at ∼5% total substrate consumption (∼0.05 μM). The acidified reaction mixture was extracted with dichloromethane, evaporated to dryness under a vacuum, reconstituted in 50 μL of MeOH, and injected onto a Phenomenex Luna (5 μm, 250 × 4.6 mm) C-18 column. The elution protocol consisted of 1 mL/min, isocratic mobile phase of 54.9% ACN/: 45% H_2O/0.1% acetic acid. The molar amount of 15-HPETE and 13-HPODE formation was calculated by the corresponding peak areas determined by the HPLC chromatogram. The ratio of the peak areas was then used to determine the $(k_{cat}/K_M)^{AA}/(k_{cat}/K_M)^{LA}$ ratio, as described in our previous report (*20*). The temperature dependency on the substrate specificity of 15-hLO-2 was determined from 15−37 °C (25 mM HEPES, pH 7.5), similar to the steady-state kinetic analysis. The pH dependency was determined from pH 6−7 (50 mM MES), from pH 7−8.5 (50 mM HEPES) and from pH 8.5−10 (50 mM CHES). Assays were performed at 37 °C and at constant ionic strength (200 mM). The 15-hLO-2 enzyme demonstrated a dramatic decrease in activity at high pH and consequently reactions performed at pH 9−10 could not be analyzed using HPLC. Therefore, product turnover at pH 9−10 was analyzed using a Finnigan LTQ liquid chromatography - tandem mass spectrometer (LC-MS/MS) as described below.

Determining the Effect of Perdeuterated 13-HODE on the pH Dependency of the Substrate Specificity of 15-hLO-2 using the Competitive Substrate Capture Method. The competitive substrate capture reactions were carried out with the addition of perdeuterated 13-HODE (5.0 μM) at pH 8.5 and pH 10 (50 mM CHES, 37 °C, ionic strength = 200 mM). The enzymatic reactions were initiated by the addition of 1 μM substrate, after preincubation of product and 15-hLO-2 (∼20 nM, normalized to iron content). The $(k_{cat}/K_M)^{AA}/(k_{cat}/K_M)^{LA}$ ratio was determined using the competitive substrate capture method as described above; however, the reduced products were quantitated with a Finnigan LTQ liquid chromatography - tandem mass spectrometer (LC-MS/MS). The titration of 13-HODE could not be performed directly since the added products would affect the $(k_{cat}/K_M)^{AA}/(k_{cat}/K_M)^{LA}$ ratio calculation by modifying their HPLC peaks. However, perdeuterated 13-HODE can be distinguished from the other LO products using LC-MS ion peaks. A Phenomenex Synergi Hydro-RP (4 μm, 150 × 2.0 mm) column was used to detect the reduced LO products with an elution protocol consisting of 0.2 mL/min, isocratic mobile phase of 59.9% ACN/40% H_2O/0.1% THF. The corresponding reduced product ion peak ratio was determined using negative ion MS/MS (collision energy = 35 eV), with the following masses: 15-HETE, parent m/z = 319, fragments m/z = 175 and 219, 12-HETE, parent m/z = 319, fragments m/z = 179 and 257, 13-HODE, parent m/z = 295, fragments m/z = 183 and 251, and perdeuterated 13-HODE, parent m/z = 325, fragments

m/z = 213 and 281 (*20*). All extracted reaction mixtures were reduced with trimethylphosphite for LC-MS/MS analysis. Similar experiments were repeated (pH 8.5) with the titration of 12-HETE for comparison to 13-HODE data.

Competitive Kinetic Isotope Effects. The variable-temperature competitive KIE for 15-hLO-2 was determined as previously described (*30−32*), using 5 μM substrate mixtures of known molar ratios (1:1) of d_{31}-LA:H-LA and d_4-AA:H-AA, in 25 mM HEPES (pH 7.5). Reactions performed with LA were initiated using 15-hLO-2 (∼40 nM) and analyzed using HPLC, whereas reactions performed with AA were initiated using 15-hLO-2 (∼20 nM) and analyzed using LC-MS/MS as previously described (*20*). Similar experiments were performed in the presence of 13-HODE (1 μM) to investigate allosteric effects on KIE.

Viscosity Studies. Viscosity studies on 15-hLO-2 (∼200− 500 nM, normalized to iron content) were performed as previously described for sLO-1 (*33, 34*). Reactions were carried out at different relative viscosities ($\eta_{rel} = \eta/\eta_o$, η_o is the viscosity of H_2O at 20 °C). Buffer and substrate solutions of 0, 21.5, and 30% by weight glucose, in 25 mM HEPES buffer (pH 7.5) were prepared corresponding to relative viscosities of 1, 2, and 3, respectively, at 20 °C. Enzymatic measurements were performed similarly as described in the steady-state kinetic analysis section. Viscosity experiments were also performed at 5 and 37 °C with AA; however, the viscosity dependency of LA could only be discerned at 37 °C, due to very low activity below physiological temperatures. Similar experiments were performed in the presence of 13-HODE (1 μM) to investigate allosteric effects on the rate-limiting nature of diffusion in the enzymatic mechanism.

Solvent Isotope Effects. The solvent isotope effect was determined by comparing the steady-state kinetic results of assays performed in H_2O and D_2O under temperatures ranging from 15−40 °C as previously described (*30, 32*). Reactions were performed in 25 mM HEPES buffer at pH = 7.5 (pH meter reading was 7.1 for D_2O), and initiated using 15-hLO-2 (∼200−500 nM, normalized to iron content). All kinetic parameters were determined as described in the steady-state kinetic section. Experiments were performed in the presence of 13-HODE (1 μM) to investigate allosteric affects on SIE.

Docking 13-HPODE/13-HODE to the Surface of a 15-hLO-2 Homology Model. The existing homology model of 15-hLO-2 from our previous publication (*20*) was employed for docking studies of 13-HODE. Similar to previous studies (*35*), flexible ligand docking of the 13-HODE was performed using the Glide (Schrödinger, Inc.) program (*36, 37*), which uses a modified version of the Chemscore energy function to score the protein−ligand interactions (*38*). The optimized force field reduces the net ionic charge on formally charged groups by ∼50% to make the gas-phase Coulombic interaction energy a better predictor of binding. The charge−charge interaction is not a qualification, but a contributor to docked poses. Molecules were docked using the extra precision mode (XP), which uses an optimized scoring function as well as an extensive search of ligand conformations.

Steady-State Inhibition Kinetics of 15-hLO-2 with d_{31}-LA. Steady-state inhibition kinetics of 15-hLO-2 (∼300 nM, normalized to iron content), with d_{31}-LA as an inhibitor, were performed as previously described (*39*). The deuterated substrate was used as an inhibitor due to its extremely slow turnover by 15-hLO-2. At the maximum inhibition concentration (100 μM), the rate of d_{31}-LA turnover was undetectable in the time frame of the
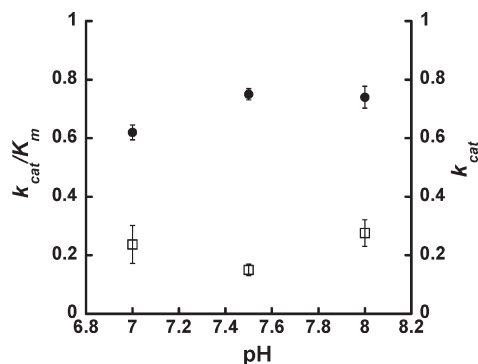
FIGURE 1: pH dependence of k_{cat}/K_M (open squares) and k_{cat} (closed circles) for 15-hLO-2 with AA. Enzymatic reactions were performed in 25 mM HEPES buffer at 22 °C.
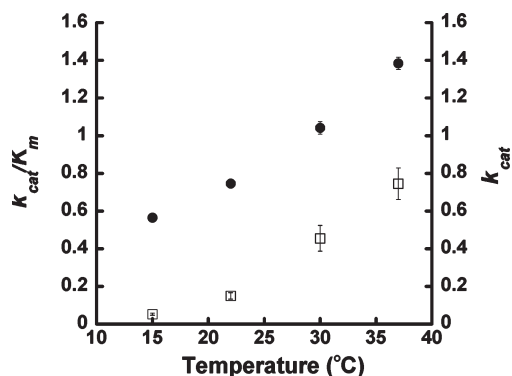

FIGURE 2: Temperature dependence of k_{cat}/K_M (open squares) and k_{cat} (closed circles) for 15-hLO-2 with AA. Enzymatic reactions were performed in 25 mM HEPES buffer at pH 7.5.

initial rate determination. Steady-state kinetic analysis was performed as described above, using d_{31}-LA concentrations of 0 μM, 25 μM, 50 μM, and 100 μM, in the presence of Triton X-100 (0.01%) to disrupt aggregate formation, as previously described (*39*). Further inhibition investigations were performed with 13-HODE (1 μM) added, at d_{31}-LA concentrations of 0 μM, 5 μM, 10 μM, and 15 μM (25 mM HEPES, pH 7.5, 0.01% Triton X-100).

RESULTS AND DISCUSSION

Mechanistic Investigations of Human 15-Lipoxygenase-2 with AA. pH Dependency of Steady-State Kinetics. The pH dependency of 15-hLO-2 activity was investigated with AA, at constant ionic strength (20 mM) and found to be approximately level between pH 7−8, similar to previously reported results for other human lipoxygenases (*32*). The k_{cat}/K_M values were determined to be 0.24 ± 0.06 μM^{-1} s^{-1}, 0.15 ± 0.02 μM^{-1} s^{-1}, and 0.28 ± 0.04 μM^{-1} s^{-1}, and k_{cat} values were determined to be 0.62 ± 0.03 s^{-1}, 0.75 ± 0.02 s^{-1}, and 0.74 ± 0.04 s^{-1}, for pH 7, pH 7.5, and pH 8.0, respectively (Figure 1). All subsequent experiments were performed at physiological pH (7.5), unless otherwise described.

Temperature Dependency of Steady-State Kinetics. 15-hLO-2 displayed temperature dependent steady-state kinetic parameters with no observable autoinactivation. The k_{cat}/K_M, normalized to iron content, was determined to be 0.05 ± 0.02 μM^{-1} s^{-1}, 0.15 ± 0.02 μM^{-1} s^{-1}, 0.46 ± 0.03 μM^{-1} s^{-1}, 0.75 ± 0.03 μM^{-1} s^{-1} for 15, 22, 30, and 37 °C, respectively (Figure 2). The k_{cat} data was determined to be 0.57 ± 0.01 s^{-1}, 0.75 ± 0.02 s^{-1}, 1.04 ± 0.07 s^{-1},
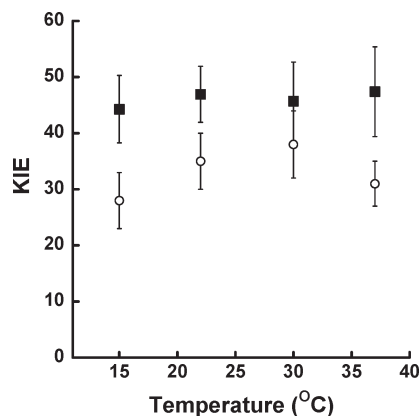

FIGURE 3: Temperature dependence of competitive KIE for 15-hLO-2: $^{D}k_{cat}/K_M$[AA] (open circle) and $^{D}k_{cat}/K_M$[LA] (closed square). Enzymatic assays were performed at 5 μM substrate concentrations in 25 mM HEPES Buffer (pH 7.5).

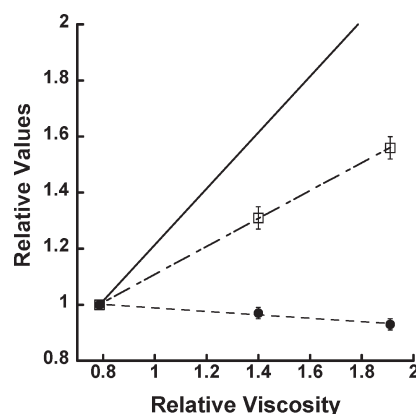FIGURE 4: Effect of relative viscosity (η/η^0) on normalized values of reciprocal k_{cat}/K_M[AA] at 37 °C. The slope of the line is 0.50 (±0.03) and −0.062 (±0.004) for k_{cat}/K_M (open circles) and k_{cat} (close circles), respectively. Solid line is the theoretical behavior for a fully diffusion controlled reaction. Enzymatic assays were performed in 25 mM HEPES buffer (pH 7.5) with 0%, 21.6%, and 30% w/v glucose.

1.38 ± 0.08 s^{-1}, for 15, 22, 30, and 37 °C, respectively. At 22 °C, the k_{cat}/K_M and k_{cat} values are in excellent agreement with previously published results (*20*).

Competitive Kinetic Isotope Effects. The KIE of 15-hLO-2 can only be determined with the competitive KIE method, due to the extremely slow reactivity with deuterated AA. The observed competitive $^{D}k_{cat}/K_M$[AA] was determined to be 28 ± 5, 35 ± 6, 38 ± 6, and 31 ± 4, at 15, 22, 30, and 37 °C, respectively (Figure 3). As seen in Figure 3, the magnitude of the $^{D}k_{cat}/K_M$[AA] for 15-hLO-2 is greater than semiclassical predictions, which is indicative of a hydrogen tunneling mechanism (*40−44*). Furthermore, there appears to be a slight temperature dependency of the $^{D}k_{cat}/K_M$[AA], possibly due to multiple rate-determining steps; however, further experiments are required to confirm this hypothesis (vide infra). To determine if allosteric binding affects the KIE of 15-hLO-2, as previously seen for 15-hLO-1 (*20, 24*), 13-HODE (1 μM) was added at 37 °C, but little effect was observed ($^{D}k_{cat}/K_M$[AA] = 33 ± 4). This result suggests that allosteric binding either does not affect the nature of the RDS or the change is so small in comparison to the observed KIE that it is not measurable.

Viscosity Studies. To probe the presence of multiple RDSs, viscosity experiments were performed as previously described for
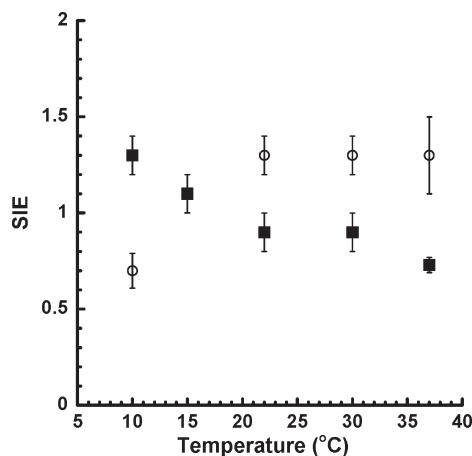
FIGURE 5: Temperature dependence of the SIE for 15-hLO-2 with AA as substrate: k_{cat} (close squares) and k_{cat}/K_M (open circles). Enzymatic assays were performed in 25 mM HEPES buffer (pH 7.5).

FIGURE 6: pH dependence of the substrate specificity for 15-hLO-2, using the competitive substrate capture. Enzymatic assays were performed at 1 μM substrate concentrations in 50 mM MES (pH 6−7), 50 mM HEPES (pH 7−8.5), 50 mM CHES (pH8 0.5−10) at 37 °C and constant ionic strength (200 mM). Fitting the data revealed a p$K_{a(app)}$ = 7.7 ± 0.1.

sLO-1 (*30, 34*). From Figure 4, the reaction rate of 15-hLO-2 with AA at 37 °C demonstrates 50 ± 3% viscosity dependence, decreasing to 35 ± 2% and 2.5 ± 0.3% at 20 and 5 °C, respectively (Figures S1 and S2, Supporting Information) indicating that diffusion is partially rate limiting in the reaction, which decreases in significance with temperature. There is a slight increase in the k_{cat}[AA] with decreasing viscosity at 37 °C (∼6.2%), which was also observed for sLO-1 (∼10%), demonstrating that the viscogen does not inhibit 15-hLO-2 (*30*). It should be noted that previous viscosity experiments with 12-hLO and 15-hLO-1 could not be performed due to inhibition by the viscogens (*32*). To test if allosteric binding affects the rate-limiting nature of the diffusion step, the viscosity dependency measurements were also performed in the presence of 13-HODE (1 μM) at 37 °C, which demonstrated no effect, within error (57 ± 5%, data not shown).

Solvent Isotope Effects. The solvent isotope effect dependency experiments demonstrated an inverted k_{cat}/K_M[AA] SIE of 0.70 ± 0.09 for 15-hLO-2 at 15 °C, which saturates at 1.3 ± 0.2, between 22−37 °C (Figure 5). The k_{cat}[AA] SIE was nearly reciprocal of the k_{cat}/K_M[AA] SIE data, demonstrating a normal solvent dependence of 1.3 ± 0.1 at 15 °C, which decreased to 0.73 ± 0.04 at 37 °C (Figure 5).

To determine if allosteric binding affects the solvent dependency of 15-hLO-2, as previously seen for 15-hLO-1 (*20*), 13-HODE (1 μM) was added to the SIE[AA] assay at 10 and 37 °C. The binding of 13-HODE abolished the SIE, demonstrating a k_{cat}[AA] SIE of 0.91 ± 0.05 and a k_{cat}/K_M[AA] SIE of 0.9 ± 0.3 at 37 °C and a k_{cat}[AA] SIE of 1.05 ± 0.09 and a k_{cat}/K_m[AA] SIE of 1.0 ± 0.2 at 10 °C. These results indicate that upon allosteric binding of 13-HODE, the rate-limiting nature of the solvent dependency is eliminated, similar to that seen for 15-hLO-1 with AA (*24*).

Summary of 15-hLO-2 with AA as Substrate. The large observed $^D k_{cat}/K_M$ that 15-hLO-2 displays for AA indicates that the H-atom abstraction occurs through a tunneling mechanism, similar to that seen for 15-hLO-1 with AA (*24*). The slight lowering of the observed KIE at high temperature appears to be due to both diffusion and hydrogen-bond rearrangements becoming increasingly rate-limiting. At low temperature, however, the nature of the RDS for k_{cat}/K_M is distinct, manifesting only a slight decrease in KIE, with little contribution from diffusion and an inverted SIE. These data suggest that the
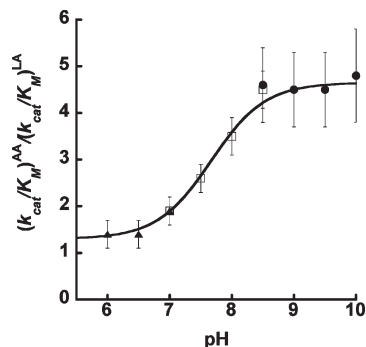
substrate capture (k_{cat}/K_M) for 15-hLO-2 with AA is rate-limited by three steps (diffusion, hydrogen bonding rearrangement, and hydrogen atom abstraction) at physiological temperature (37 °C); however, the small temperature dependence of $^D k_{cat}/K_M$ is perplexing since the large effect in viscosity and in SIE would have suggested a greater effect should be observed, as seen for sLO-1 (*30*). This muted temperature dependence was also observed with the addition of 13-HODE, which removed the SIE but did not affect the observed $^D k_{cat}/K_M$. We currently do not have a biochemical explanation for this discrepancy, but we partially attribute it to the inherent degree of error in our LC-MS method as compared to the HPLC method. We are currently optimizing our LC-MS method in the hopes of probing these results further.

With respect to the inverted SIE with AA as substrate, our laboratory previously observed an inverted SIE with a sLO-1 mutant, Q697E, which we interpreted as being due to the catalytic Fe^{III}-OH species, which abstracts the hydrogen atom (*45*). This explanation appears not to be appropriate for 15-hLO-2 since the allosteric effector, 13-HODE, reverts the SIE to unity but does not affect the KIE value. If the inverted SIE were due to the Fe^{III}-OH species of 15-hLO-2, then the rate-limiting nature of the abstraction (i.e., the KIE) should decrease as the magnitude of the inverted SIE changes since they are due to the same chemical species, the Fe^{III}-OH. This was not observed, so the inverted SIE appears to be due to a different chemical species than the Fe^{III}-OH. In the literature, inverted SIEs are most commonly associated with nucleophilic cysteines (*46−48*), but no cysteines have been implicated in the mechanism of the LO family of isozymes, even though there are two cysteine residues in the active site of the 15-hLO-2 homology model, C549 and C564, with the former being conserved within most human LOs. Inverse SIE values can also be caused by thermodynamic effects (*49, 50*). The acid dissociation constants of D_2O and H_2O can be different, with the pK_a of some amino acid side chains increasing as much as ∼0.4 units in D_2O. If a critical amino acid is partially protonated (its pK_a being slightly below the pH of the SIE experiment, pH = 7.5), then in D_2O the residue will be partially deprotonated, which could affect the enzymatic rate and lead to an inverse SIE. Another possible explanation is that in the absence of 13-HODE, 15-hLO-2 is partially unfolded at low temperatures, which could potentially have a different fractionation factor than the folded state (the fractionation factor of a hydrogen bonded amide backbone is approximately 1.1 (*51*)). If the binding of 13-HODE
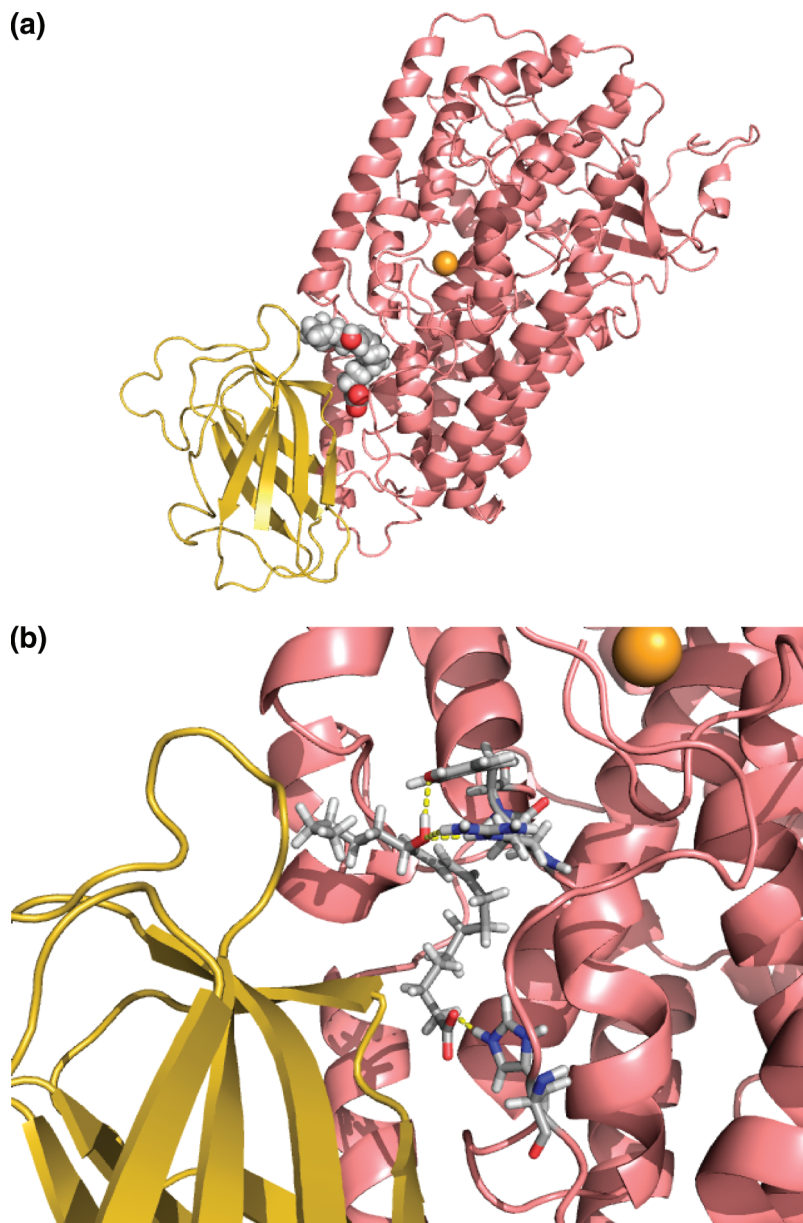
(a)

(b)

FIGURE 7: (a) 15-hLO-2 homology model docked with 13-HODE (space filling model) in the proposed allosteric site. Figure generated with Pymol. (b) Magnified view of 15-hLO-2 homology model docked with 13-HODE (stick model) in the proposed allosteric site, depicting hydrogen bonding interactions of the carboxylate of 13-HODE with H627 and its alcohol moiety with R407 and Y408. Figure generated with Pymol.

leads to a conformational change which results in the formation of a strong hydrogen bond, then this step could lead to an inverse SIE (*52, 53*). We are currently investigating these hypotheses further with pH dependence, proton inventory, mutational and denaturation experiments, in the hopes of understanding the inverse SIE in more detail.

Mechanistic Investigations of Human 15-Lipoxygenase-2 with LA. Competitive Kinetic Isotope Effects. The observed competitive $^D k_{cat}/K_M$ values for 15-hLO-2 with LA were determined to be approximately temperature independent, with an average $^D k_{cat}/K_M[LA]$ value of 45 ± 3 (Figure 3); however, there is a high degree of error in each individual temperature point, which could mask a slight temperature dependence. Unfortunately, performing steady-state viscosity and solvent dependency measurements to confirm the presence of multiple rate-limiting steps is not possible due to the low rate of reaction (k_{cat}) with LA. A high concentration of enzyme is required for LA kinetics, which approaches the substrate con-

centration and consequently leads to kinetic conditions that violate the steady-state approximation. Nonetheless, the magnitude of the observed $^D k_{cat}/K_M[LA]$ indicates that the hydrogen atom abstraction occurs through a tunneling mechanism, as seen with AA.

Substrate Specificity and Allosteric Binding Investigations. Temperature and pH Dependency Studies. The $(k_{cat}/K_M)^{AA}/(k_{cat}/K_M)^{LA}$ ratio was determined to be temperature independent (2.1 ± 0.1 at 15 °C, 2.2 ± 0.2 at 22 °C, 2.5 ± 0.2 at 30 °C and 2.4 ± 0.1 at 37 °C (25 mM HEPES, pH 7.5, ionic strength = 200 mM)); however, the $(k_{cat}/K_M)^{AA}/(k_{cat}/K_M)^{LA}$ ratio did show a significant dependence on pH (Figure 6).

The $(k_{cat}/K_M)^{AA}/(k_{cat}/K_M)^{LA}$ ratio increased from 1.4 ± 0.3 at pH 6.0 to 4.5 ± 0.5, at pH 10 (Figure 6). This value is lower than that observed with steady-state kinetics ($(k_{cat}/K_M)^{AA}/(k_{cat}/K_M)^{LA}$ ratio = 8 ± 1 (*20*), which we attribute to the inaccuracies of the steady-state method. As stated above, the amount of 15-hLO-2 needed for measurable rates with LA as substrate is such
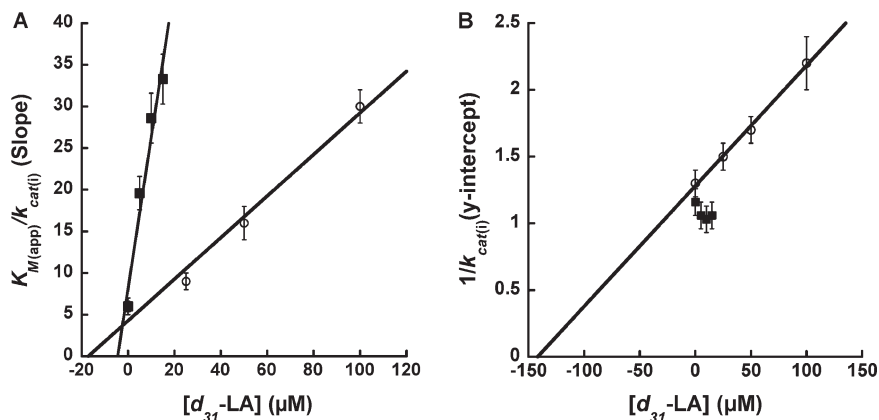
FIGURE 8: Steady-state inhibition kinetics data for the determination of K_i and K_i' for 15-hLO-2 with d_{31}-LA as an inhibitor, with and without 13-HODE addition. (A) $K_{M(app)}/k_{cat(i)}$ (slope) versus $[d_{31}$-LA$] \mu$M is the secondary replot of inhibition data used to determine K_i. Without 13-HODE addition $K_i = 17 \pm 3 \mu$M (open circles) and with 13-HODE addition (1 μM) $K_i = 5 \pm 1 \mu$M (closed squares). (B) $1/k_{cat(i)}$ (y-intercept) versus d_{31}-LA μM is a secondary replot of inhibition data used to determine K_i'. Without 13-HODE addition $K_i' = 149 \pm 10 \mu$M (open circles) and with 13-HODE addition K_i' is not observed (closed squares). Enzymatic assays were performed in 25 mM HEPES (pH 7.5) at 22 °C with AA as substrate.

that it is of comparable concentration as the substrate, leading to a high degree of error. Therefore, we consider the value of 4.5 ± 0.5 to be more accurate since it was done with our competitive method. The pK_a value was determined by fitting the data to eq 1 (Figure 6), which is derived from a simple acid dissociation equilibrium (*54*):

$$Y = (1.3 + (4.65 \times 10^{(X-Z)}))/(1 + 10^{(X-Z)}) \qquad (1)$$

where 1.3 and 4.65 are the end points of the fit, Y is the $(k_{cat}/K_M)^{AA}/(k_{cat}/K_M)^{LA}$ ratio, X is the pH of the system and Z is the calculated pK_a. The fitted data from Figure 6 indicates a $pK_{a(app)} = 7.7 \pm 0.1$.

This observed pH dependency of the substrate specificity, coupled with our previous data which demonstrated that perdeuterated 13-HPOD, at pH 7.5, had no effect on the substrate specificity ratio, lead us to suspect that pH may be affecting the binding affinity of 13-HODE to the allosteric site, presumably via a hydrogen bonding interaction. To test this hypothesis, perdeuerated 13-HODE (100 nM) was added at pH 8.5 and pH 10, and the $(k_{cat}/K_M)^{AA}/(k_{cat}/K_M)^{LA}$ decreased from 4.6 ± 0.8 to 1.8 ± 0.3 and from 4.8 ± 1.0 to 1.9 ± 0.3, respectively. This effect was not seen with the addition of 2 μM of 12-HETE (pH 8.5), supporting the hypothesis that 13-HODE binding to the allosteric site is affecting this change.

The above data allows an approximation of the binding coefficient of 13-HODE to the allosteric site at the two extremes of the pH titration curve. Given that the addition of 13-HODE has no effect on the substrate specificity at pH 7.5 and below, and that the AA/LA ratio is markedly greater under steady-state conditions (*20*), these data suggest that the allosteric site is saturated. Since the competitive assay is stopped at 50 nM product production (5% of 1 μM) and 13-HODE is only 40% of the total product formed $((k_{cat}/K_M)^{AA}/(k_{cat}/K_M)^{LA} = 1.5)$, then the maximal concentration of 13-HODE in solution is 20 nM. Since the site appears to be saturated at this 13-HODE concentration, then we estimate the K_D to be approximately 5 nM. This value is at least 200-fold less than that of 13-HODE binding to 15-hLO-1, which is 1 μM (*20*). At pH 8.5 and above, 100 nM of 13-HODE is sufficient to saturate the allosteric site, suggesting a K_D of approximately 50 nM. This approximate 10-fold difference in K_D upon pH titration of 15-hLO-2 represents a $\Delta G°$ of ~1.4 kcal/mol. This value, along with the pK_a of the titration curve

$(pK_{a(app)} = 7.7 \pm 0.1)$, is consistent with a solvent exposed histidine hydrogen bonding to the carboxylate of the 13-HODE.

Docking 13-HPODE/13-HODE to the 15-hLO-2 Homology Model. Assuming the protonation state of a solvent exposed histidine was responsible for the varying affinity of 13-HPODE/13-HODE, a 15-hLO-2 homology model was employed to determine the location of the allosteric site. Visual analysis of the homology model enabled the selection of seven solvent exposed histidines to be used in a docking study (H160, H368, H376, H394, H396, H405, H411, and H627). The protonation state of the seven histidines was altered manually to provide the overall +1 charge on the histidine side chain in the 15-hLO-2 homology model. Separate docking grids were created for each of the seven histidines and 13-HPODE was docked to each corresponding model. Only three models were able to accommodate 13-HPODE in the alternative binding pockets based on the grids centered around H376, H394, and H627. Of these, only the poses centered on H627 provided an interaction between the carboxylic moiety of 13-HPODE and the +1 charged histidine. 13-HODE was also docked to this site and found to have an additional bifurcated hydrogen bond with residue R407 and Y408 (Figure 7).

Steady-State Inhibition Kinetics of 15-hLO-2 with d_{31}-LA. As discussed in Materials and Methods, 15-hLO-2 activity against d_{31}-LA is undetectable in the time frame of our steady-state experiments. Therefore, d_{31}-LA was utilized as an inhibitor for steady-state inhibition studies, allowing the $K_{M(app)}$ and $k_{cat(app)}$ values with AA as substrate to be obtained at various d_{31}-LA concentrations (plots not shown). The addition of d_{31}-LA manifested linear mixed-type inhibition toward 15-hLO-2, demonstrating a K_i and K_i' (*55*). The K_i and K_i' are defined as the equilibrium constants for the dissociation of inhibitor from the catalytic site and a secondary site (presumably the allosteric site), respectively (*15, 20*). The $K_{M(app)}/k_{cat(i)}$ versus $[d_{31}$-LA$] \mu$M plot yielded a K_i of $17 \pm 3 \mu$M, and the $1/k_{cat(i)}$ versus $[d_{31}$-LA$]$ plot yielded a K_i' of $149 \pm 10 \mu$M (Figure 8, panels A and B, respectively), indicating a nearly 10-fold difference in affinities between the catalytic and secondary site.

To test whether the secondary binding site of LA is the same as the allosteric binding site, the inhibition studies were also performed in the presence of 13-HODE (1 μM) to saturate the allosteric site (pH 7.5). The data demonstrated that the mode of inhibition of d_{31}-LA, in the presence of 13-HODE, changed from

mixed-type inhibition to competitive inhibition with a K_i of 5 ± 1 μM (Figure 8A,B). Considering that the K_D of 13-HODE for the allosteric site is approximately 5 nM (pH 7.5), there is nearly a 30 000-fold difference in affinity for the allosteric site between 13-HODE and the substrate, LA ($\sim$5 nM vs $\sim$150 μM, respectively). This is remarkable given the structural similarities between 13-HODE and LA; however, it is consistent with our previous result which showed the allosteric site in sLO-1 discriminating between similar inhibitors, oleyl sulfate and palmitoleoyl sulfate, by $\sim$230-fold (*56*). This result is also consistent with our allosteric binding model, which demonstrates hydrogen bonds between the 13-HODE alcohol and R407/Y408, which is not possible with LA. Furthermore, the binding of 13-HODE to the allosteric site decreased the K_i from 17 ± 3 μM to 5 ± 1 μM, which corroborates our previous observation of a nearly 2-fold decrease in the K_M for LA with 13-HPODE activated enzyme (*20*). This result indicates that the allosteric effector, 13-HODE, changes the conformation of 15-hLO-2 such that substrate affinity toward LA is significantly increased. These findings are distinct from the findings of COX, which manifests a change in conformation only after substrate binding (*57*).

CONCLUSION

Our laboratory has been interested in the allosteric regulation of LO activity since our initial discovery of the allosteric site on sLO-1 and 15-hLO-1 (*15*). Since the original findings, we have demonstrated the existence of an allosteric, product-feedback loop which directly affects the substrate specificity of both 15-hLO-1 and 15-hLO-2 (*20*). In the case of 15-hLO-1, the allosteric effector not only changes the substrate specificity but also the nature of the rate-limiting contributions of the individual steps in the reaction mechanism (*24*). In the current work, we have extended this investigation to 15-hLO-2 and present isotopic effect, pH, and substrate inhibitor data, which probe the allosteric affects on the functional behavior of 15-hLO-2.

The $^{D}k_{cat}/K_M$ for 15-hLO-2, with AA and LA as substrate, is large indicating hydrogen atom abstraction as a principal RDS and that there is a tunneling mechanism for both substrates. In addition, there are multiple RDSs for AA at both high and low temperature, with both diffusion and hydrogen bonding rearrangements contributing at high temperature, but only hydrogen bonding rearrangements contributing at low temperature. The observed kinetic dependency on the hydrogen bonding rearrangement is eliminated upon addition of the allosteric effector, 13-HODE, and no allosteric; however, no allosteric effects were seen on diffusion or hydrogen atom abstraction. These results are similar to those with 15-hLO-1, which also manifests a solvent dependency of the RDS, which is eliminated upon binding of an allosteric effector (12-HETE), suggesting that the structural change upon allosteric effector binding may be similar between the two isozymes. Interestingly, the allosteric site conformation changes of 15-hLO-2 not only affect the solvent dependency of the RDS, but also the affinity for substrate, as seen by the decrease in K_i for d_{31}-LA. These results corroborate our original findings which demonstrated that the addition of 13-HODE increased the k_{cat}/K_M of LA (*20*). We speculate that allosteric binding may be locking the enzyme into a catalytically competent state, which facilitates binding of LA and decreases the $(k_{cat}/K_M)^{AA}/(k_{cat}/K_M)^{LA}$ ratio.

A notable difference between the allosteric behavior between 15-hLO-1 and 15-hLO-2 is the pH dependence of their substrate specificity. For 15-hLO-1, there is no effect of pH (data not shown), but for 15-hLO-2, there is a large pH effect. In fact, the pH dependency can be fit with a titration curve ($pK_a = 7.7$), suggesting the protonation of a histidine residue, which could hydrogen bond with the carboxylate of 13-HODE. Assuming this interaction, 13-HODE was docked to the solvent exposed histidines of our 15-hLO-2 homology model and found to have a chemically reasonable interaction with H627 (Figure 7B). This proposed allosteric site is $\sim$15 Å from the edge of the active site and is located between the two domains, which could affect the enzymatic activity through domain−domain interactions, since removal of the beta-domain has been shown to affect sLO-1 catalysis (*58*). We are currently generating mutants of H627, R407, and Y408, in order to confirm or refute the location of the allosteric site and its molecular mechanism for changing substrate specificity.

Finally, the magnitude of the 13-HODE K_D for 15-hLO-2 is over 200-fold lower than that of 12-HETE and 13-HODE for 15-hLO-1. This observation may have important implications in the cell since very small amounts of 13-HODE have large effects on the substrate specificity of 15-hLO-2. It has been hypothesized that 15-hLO-2 is antitumorigenic due to its high level of expression in normal tissue (*59*) and the fact that 15-hLO-2 produces mainly 15-HETE ($(k_{cat}/K_M)^{AA}/(k_{cat}/K_M)^{LA}$ ratio = 4.5), which is antitumorigenic (*60, 61*). Interestingly, the current data indicate that at small levels of 13-HODE (5 nM), the $(k_{cat}/K_M)^{AA}/(k_{cat}/K_M)^{LA}$ ratio of 15-hLO-2 changes to 1.9, which would alter the LO product distribution by increasing the production of the pro-tumorigenic 13-HPODE (*61, 62*). This effect possibly represents a pro-tumorigenic feedback loop for 13-HODE against 15-hLO-2, which we are currently investigating directly in cancer cells.

ACKNOWLEDGMENT

SUPPORTING INFORMATION AVAILABLE

Determination of the viscosity dependency on the steady-state kinetics of 15-hLO-2 at 20 and 5 °C. This material is available free of charge via the Internet at http://pubs.acs.org.

REFERENCES

1. Vane, J. R., Bakhle, Y. S., and Botting, R. M. (1998) Cyclooxygenases 1 and 2. *Annu. Rev. Pharmacol. Toxicol. 38*, 97–120.
2. Capdevila, J. H., Falck, J. R., and Estabrook, R. W. (1992) Cytochrome P450 and the arachidonic cascade. *FASEB J. 6*, 731–736.
3. Haeggstrom, J. Z., and Wetterholm, A. (2002) Enzymes and receptors in the leukotriene cascade. *Cell. Mol. Life Sci. 59*, 742–753.
4. Yamamoto, S. (1992) Mammalian lipoxygenases: molecular structures and functions. *Biochim. Biophys. Acta 1128*, 117–131.
5. Solomon, E. I., Zhou, J., Neese, F., and Pavel, E. G. (1997) New insights from spectroscopy into the structure/function relationships of lipoxygenases. *Chem. Biol. 4*, 795–808.
6. Serhan, C. N. (1994) Lipoxin biosynthesis and its impact in inflammatory and vascular events. *Biochim. Biophys. Acta 1212*, 1–25.
7. Nakano, H., Inoue, T., Kawasaki, N., Miyataka, H., Matsumoto, H., Taguchi, T., Inagaki, N., Nagai, H., and Satoh, T. (2000) Synthesis and biological activities of novel antiallergic agents with 5-lipoxygenase inhibiting action. *Bioorg. Med. Chem. 8*, 373–380.
8. Hussain, H., Shornick, L. P., Shannon, V. R., Wilson, J. D., Funk, C. D., Pentland, A. P., and Holtzman, M. J. (1994) Epidermis contains platelet-type 12-lipoxygenase that is overexpressed in germinal layer keratinocytes in psoriasis. *Am. J. Physiol. 266*, C243–253.
9. Harats, D., Shaish, A., George, J., Mulkins, M., Kurihara, H., Levkovitz, H., and Sigal, E. (2000) Overexpression of 15-lipoxygenase in vascular endothelium accelerates early atherosclerosis in LDL

receptor-deficient mice. *Arterioscler. Thromb. Vasc. Biol. 20*, 2100–2105.

10. Steele, V. E., Holmes, C. A., Hawk, E. T., Kopelovich, L., Lubet, R. A., Crowell, J. A., Sigman, C. C., and Kellof, G. J. (1999) Lipoxygenase inhibitors as potential cancer chemopreventives. *Cancer Epidemiol., Biomarkers Prevention 8*, 467–483.

11. Falgueyret, J. P., Denis, D., Macdonald, D., Hutchinson, J. H., and Riendeau, D. (1995) Characterization of the arachidonate and ATP binding sites of human 5-lipoxygenase using photoaffinity labeling and enzyme immobilization. *Biochemistry 34*, 13603–13611.

12. Hogaboom, G. K., Cook, M., Newton, J. F., Varrichio, A., Shorr, R. G., Sarau, H. M., and Crooke, S. T. (1986) Purification, characterization, and structural properties of a single protein from rat basophilic leukemia (RBL-1) cells possessing 5-lipoxygenase and leukotriene A4 synthetase activities. *Mol. Pharmacol. 30*, 510–519.

13. Rouzer, C. A., and Samuelsson, B. (1986) The importance of hydroperoxide activation for the detection and assay of mammalian 5-lipoxygenase. *FEBS Lett. 204*, 293–296.

14. Shimizu, T., Izumi, T., Seyama, Y., Tadokoro, K., Radmark, O., and Samuelsson, B. (1986) Characterization of leukotriene A4 synthase from murine mast cells: evidence for its identity to arachidonate 5-lipoxygenase. *Proc. Natl. Acad. Sci. U. S. A. 83*, 4175–4179.

15. Mogul, R., Johansen, E., and Holman, T. R. (2000) Oleyl sulfate reveals allosteric inhibition of soybean lipoxygenase-1 and human 15-lipoxygenase. *Biochemistry 39*, 4801–4807.

16. Ruddat, V. C., Whitman, S., Holman, T. R., and Bernasconi, C. F. (2003) Stopped-flow kinetic investigations of the activation of soybean lipoxygenase-1 and the influence of inhibitors on the allosteric site. *Biochemistry 42*, 4172–4178.

17. Shappell, S. B., Manning, S., Boeglin, W. E., Guan, Y. F., Roberts, R. L., Davis, L., Olson, S. J., Jack, G. S., Coffey, C. S., Wheeler, T. M., Breyer, M. D., and Brash, A. R. (2001) Alterations in lipoxygenase and cyclooxygenase-2 catalytic activity and mRNA expression in prostate carcinoma. *Neoplasia 3*, 287–303.

18. Butler, R. M., S., H., Tindall, D. J., and Young, C. Y. (2000) Nonapoptotic cell death associated with S-phase arrest of prostate cancer cells via the peroxisome proliferator-activated receptor gamma ligand, 15-deoxy-delta12,14-prostaglandin J2. *Cell Growth Differ. 11*, 49–61.

19. Hsi, L. C., Wilson, L., Nixon, J., and Eling, T. E. (2001) 15-Lipoxygenase-1 metabolites down-regulate peroxisome proliferator-activated receptor gamma via the MAPK signaling pathway. *J. Biol. Chem. 276*, 34545–34552.

20. Wecksler, A. T., Kenyon, V., Deschamps, J. D., and Holman, T. R. (2008) Substrate specificity changes for human reticulocyte and epithelial 15-lipoxygenases reveal allosteric product regulation. *Biochemistry 47*, 7364–7375.

21. Nordlund, P., and Reichard, P. (2006) Ribonucleotide reductases. *Annu. Rev. Biochem. 75*, 681–706.

22. Reichard, P. (2002) Ribonucleotide reductases: the evolution of allosteric regulation. *Arch. Biochem. Biophys. 397*, 149–155.

23. Guichardant, M., Thevenon, C., Pageaux, J. F., and Lagarde, M. (1997) Basal concentrations of free and esterified monohydroxylated fatty acids in human blood platelets. *Clin. Chem. 43*, 2403–2407.

24. Wecksler, A. T., Jacquot, C., van der Donk, W. A., and Holman, T. R. (2009) Mechanistic investigations of human reticulocyte 15- and platelet 12-lipoxygenases with arachidonic acid. *Biochemistry 48*, 6259–6267.

25. Lewis, E., Johnson, E., and Holman, T. (1999) Large competitive kinetic isotope effects in human 15-lipoxygenase catalysis measured by a novel HPLC method. *J. Am. Chem. Soc. 121*, 1395–1396.

26. Jacquot, C., Wecksler, A. T., McGinley, C. M., Segraves, E. N., Holman, T. R., and van der Donk, W. A. (2008) Isotope sensitive branching and kinetic isotope effects in the reaction of deuterated arachidonic acids with human 12- and 15-lipoxygenases. *Biochemistry 47*, 7295–7303.

27. Peng, S., Okeley, N. M., Tsai, A. L., Wu, G., Kulmacz, R. J., and van der Donk, W. A. (2002) Synthesis of isotopically labeled arachidonic acids to probe the reaction mechanism of prostaglandin H synthase. *J. Am. Chem. Soc. 124*, 10785–10796.

28. Peng, S., McGinley, C. M., and van der Donk, W. A. (2004) Synthesis of site-specifically labeled arachidonic acids as mechanistic probes for prostaglandin H synthase. *Org. Lett. 6*, 349–352.

29. Deschamps, J. D., Gautschi, J. T., Whitman, S., Johnson, T. A., Gassner, N. C., Crews, P., and Holman, T. R. (2007) Discovery of platelet-type 12-human lipoxygenase selective inhibitors by high-throughput screening of structurally diverse libraries. *Bioorg. Med. Chem. 15*, 6900–6908.

30. Glickman, M. H., and Klinman, J. P. (1995) Nature of rate-limiting steps in the soybean lipoxygenase-1 reaction. *Biochemistry 34*, 14077–14092.

31. Rickert, K. W., and Klinman, J. P. (1999) Nature of hydrogen transfer in soybean lipoxygenase 1: separation of primary and secondary isotope effects. *Biochemistry 38*, 12218–12228.

32. Segraves, E. N., and Holman, T. R. (2003) Kinetic investigations of the rate-limiting step in human 12- and 15-lipoxygenase. *Biochemistry 42*, 5236–5243.

33. Glickman, M. H., and Klinman, J. P. (1996) Lipoxygenase reaction mechanism: demonstration that hydrogen abstraction from substrate precedes dioxygen binding during catalytic turnover. *Biochemistry 35*, 12882–12892.

34. Jacquot, C., Peng, S., and van der Donk, W. A. (2008) Kinetic isotope effects in the oxidation of arachidonic acid by soybean lipoxygenase-1. *Bioorg. Med. Chem. Lett. 18*, 5959–5962.

35. Kenyon, V., Chorny, I., Carvajal, W. J., Holman, T. R., and Jacobson, M. P. (2006) Novel human lipoxygenase inhibitors discovered using virtual screening with homology models. *J. Med. Chem. 49*, 1356–1563.

36. Friesner, R. A., Banks, J. L., Murphy, R. B., Halgren, T. A., Klicic, J. J., Mainz, D. T., Repasky, M. P., Knoll, E. H., Shelley, M., Perry, J. K., Shaw, D. E., Francis, P., and Shenkin, P. S. (2004) Glide: A new approach for rapid, accurate docking and scoring. 1. Method and assessment of docking accuracy. *J. Med. Chem. 47*, 1739–1749.

37. Halgren, T. A., Murphy, R. B., Friesner, R. A., Beard, H. S., Frye, L. L., Pollard, W. T., and Banks, J. L. (2004) Glide: A new approach for rapid, accurate docking and scoring. 2. Enrichment factors in database screening. *J. Med. Chem. 47*, 1750–1759.

38. Eldridge, M. D., Murray, C. W., Auton, T. R., Paolini, G. V., and Mee, R. P. (1997) Empirical scoring functions: I. The development of a fast empirical scoring function to estimate the binding affinity of ligands in receptor complexes. *J. Comput. Aided Mol. Des. 11*, 425–445.

39. Deschamps, J. D., Kenyon, V. A., and Holman, T. R. (2006) Baicalein is a potent in vitro inhibitor against both reticulocyte 15-human and platelet 12-human lipoxygenases. *Bioorg. Med. Chem. 14*, 4295–4301.

40. Klinman, J. P. (2006) The role of tunneling in enzyme catalysis of C-H activation. *Biochim. Biophys. Acta 1757*, 981–987.

41. Knapp, M. J., and Klinman, J. P. (2002) Environmentally coupled hydrogen tunneling. Linking catalysis to dynamics. *Eur. J. Biochem. 269*, 3113–3121.

42. Knapp, M. J., Rickert, K., and Klinman, J. P. (2002) Temperature-dependent isotope effects in soybean lipoxygenase-1: correlating hydrogen tunneling with protein dynamics. *J. Am. Chem. Soc. 124*, 3865–3874.

43. Edwards, S. J., Soudackov, A. V., and Hammes-Schiffer, S. (2009) Analysis of kinetic isotope effects for proton-coupled electron transfer reactions. *J. Phys. Chem. A* xxx.

44. Kiefer, P. M., and Hynes, J. T. (2004) Kinetic isotope effects for nonadiabatic proton transfer reactions in a polar environment. 1. Interpretation of tunneling kinetic isotopic effects. *J. Phys. Chem. A 108*, 11793–11808.

45. Tomchick, D. R., Phan, P., Cymborowski, M., Minor, W., and Holman, T. R. (2001) Structural and functional characterization of second-coordination sphere mutants of soybean lipoxygenase-1. *Biochemistry 40*, 7509–7517.

46. Zhang, Z., Harms, E., and Van Etten, R. L. (1994) Asp129 of low molecular weight protein tyrosine phosphatase is involved in leaving group protonation. *J. Biol. Chem. 269*, 25947–25950.

47. Mejillano, M. R., Shivanna, B. D., and Himes, R. H. (1996) Studies on the nocodazole-induced GTPase activity of tubulin. *Arch. Biochem. Biophys. 336*, 130–138.

48. Schneck, J. L., Villa, J. P., McDevitt, P., McQueney, M. S., Thrall, S. H., and Meek, T. D. (2008) Chemical mechanism of a cysteine protease, cathepsin C, as revealed by integration of both steady-state and pre-steady-state solvent kinetic isotope effects. *Biochemistry 47*, 8697–8710.

49. Quinn, D. M., Sutton, L. D. (1991) Enzyme Mechanism from Isotope Effects , CRC Press, Boca Raton, Fl.

50. Relyea, H. A., Vrtis, J. M., Woodyer, R., Rimkus, S. A., and van der Donk, W. A. (2005) Inhibition and pH dependence of phosphite dehydrogenase. *Biochemistry 44*, 6640–6649.

51. Bowers, P. M., and Klevit, R. E. (2000) Hydrogen bond geometry and 2H/1H fractionation in proteins. *J. Am. Chem. Soc. 122*, 1030–1033.

52. Lin, J., Westler, W. M., Cleland, W. W., Markley, J. L., and Frey, P. A. (1998) Fractionation factors and activation energies for exchange of the low barrier hydrogen bonding proton in peptidyl

trifluoromethyl ketone complexes of chymotrypsin. *Proc. Natl. Acad. Sci. U.S.A. 95*, 14664–14668.

53. Kreevoy, M. M., and Liang, T. M. (2002) Structures and isotopic fractionation factors of complexes, A1HA2. *J. Am. Chem. Soc. 102*, 3315–3322.

54. Cosgrove, M. S., Loh, S. N., Ha, J. H., and Levy, H. R. (2002) The catalytic mechanism of glucose 6-phosphate dehydrogenases: assignment and 1H NMR spectroscopy pH titration of the catalytic histidine residue in the 109 kDa Leuconostoc mesenteroides enzyme. *Biochemistry 41*, 6939–6945.

55. Segal, I. H. (1993) Enzyme Kinetics: Behavior and Analysis of Equilibrium and Steady-State Enzyme Systems , John Wiley & Sons, Inc., New York.

56. Mogul, R., and Holman, T. R. (2001) Inhibition studies of soybean and human 15-lipoxygenases with long-chain alkenyl sulfate substrates. *Biochemistry 40*, 4391–4397.

57. Thuresson, E. D., Lakkides, K. M., and Smith, W. L. (2000) Different catalytically competent arrangements of arachidonic acid within the cyclooxygenase active site of prostaglandin endoperoxide H synthase-1 lead to the formation of different oxygenated products. *J. Biol. Chem. 275*, 8501–8507.

58. Di Venere, A., Salucci, M. L., van Zadelhoff, G., Veldink, G., Mei, G., Rosato, N., Finazzi-Agro, A., and Maccarrone, M. (2003) Structure-to-function relationship of mini-lipoxygenase, a 60-kDa fragment of soybean lipoxygenase-1 with lower stability but higher enzymatic activity. *J. Biol. Chem. 278*, 18281–18288.

59. Shappell, S. B. B., W., E., Olson, S. J., Kasper, S., and Brash, A. R. (1999) 15-lipoxygenase-2 (15-LOX-2) is expressed in benign prostatic epithelium and reduced in prostate adenocarcinoma. *J. Am. Pathol. 155*, 235–245.

60. Tang, D. G., Bhatia, B., Tang, S., and Schneider-Broussard, R. (2007) 15-lipoxygenase 2 (15-LOX2) is a functional tumor suppressor that regulates human prostate epithelial cell differentiation, senescence, and growth (size). *Prostaglandins Other Lipid Mediat 82*, 135–146.

61. Hsi, L. C., Wilson, L. C., and Eling, T. E. (2002) Opposing effects of 15-lipoxygenase-1 and -2 metabolites on MAPK signaling in prostate. Alteration in peroxisome proliferator-activated receptor gamma. *J. Biol. Chem. 277*, 40549–40556.

62. Schewe, T. (2002) 15-lipoxygenase-1: a prooxidant enzyme. *Biol. Chem. 383*, 365–374.